Detector based on the energy of filtered noise

Vincent Savaux

IET Research Journals

Submission Template for IET Research Journal Papers

Detector based on the energy of filtered noise

ISSN 1751-8644
doi: 0000000000
www.ietdl.org

Vincent Savaux[1]

[1] *Network Interfaces Lab, IRT b<>com, Rennes, France*
* *E-mail: vincent.savaux@b-com.com*

Abstract: This paper deals with the detection of unknown signals in white noise. We present a new detector, based on the difference of a deterministic function of the energy of the signal and the energy of the same signal, which has been filtered. Unlike usual energy detector (ED), the proposed detector consists in exploiting the behavior of the energy of filtered white noise, which can be *a priori* determined since the used filter is known. Thus, if the measured energy differs from an expected value, the detector decides that a signal is present in the band. In order to have the same asymptotic complexity as ED, a simple two-tap filter is used. The theoretical expressions of the probabilities of detection and false alarm are developed, and the optimal threshold is deduced. Simulations show that the proposed detector achieves better performance than ED, in both additive white Gaussian noise (AWGN) and Rayleigh channels. Furthermore, the relevance of the analytical results is proved through simulations.

1 Introduction

Energy detector (ED) is undoubtedly the most popular method for signal detection in noise, mainly due to its simplicity. Furthermore, it is a signal-agnostic approach, in the sense that ED does not require prior information about the signal to be detected, unlike match-filter [1], or cyclostationarity-based detectors [2]. Thus, ED is implemented in many applications, such as radar detection [3], [4], or in cognitive radio systems [5], [6], [7], [8]. In the latter application, ED may be used by secondary users in order to detect the presence of primary users in licensed bands. Secondary users can then opportunistically access the detected free bands. A large number of other sensing techniques are available in the literature, as described in [5], [6], [7], [8]. Among others, usual techniques are matched-filter [1], cyclostationarity detector [9], [10], and methods based on random matrix theory [11], [12]. However, in this paper, we will focus on energy-based detection.

The principle of ED is based on binary decision, i.e. the energy of the scanned band is compared with a threshold [13], [14]: a signal is supposed to be present (resp. absent) in the band if the energy is higher (resp. lower) than the threshold. However, setting an accurate threshold value requires the prior knowledge of the noise energy or the signal-to-noise ratio (SNR). Therefore, the performance of ED is inherently limited due to noise uncertainty [15], [16], [17]. In order to improve the performance of classical ED, several techniques have been proposed, such as described in [18] and references therein. Moreover, ED can be used in order to reduce the complexity of signal feature-based detectors. Thus, authors in [19], [20] propose to exploit benefit of both ED and second order moment-based detectors such as cyclostationarity and correlation detectors. In any case, the idea behind detection is to take advantage of the features of the signal (e.g. the energy, the shape, or redundancy of the signal) to decide if the signal is present or not.

In this paper, we examine the issue of energy detection with another paradigm, as we focus on the properties of the Gaussian white noise at the output of the receiver front-end, whereas the usual paradigm is to focus on the energy of received samples in presence of "useful" signal. Thus, the power spectral density (PSD) of white noise can be considered as constant over the whole frequency band that is sensed [13], [17]. Therefore, in absence of signal, it is possible to deduce in advance the energy of the noise after any filtering process downstream of the front-end, since the used filter is known. Such a deterministic behavior can then be used as a base for a detector. In fact, in presence of a useful signal in the noise, the measured energy of the filtered received signal differs from the expected energy based on the assumption of white noise only. This allows us to decide if the signal is present in the band or not.

Based on the previous considerations, the basic principle of the proposed detector can be summarized as follows: i) Measure the energy of the received sampled signal at the output of the front-end, and deduce the corresponding energy of the signal at the output of a predefined filter, based on the assumption that the received signal is only composed of white noise, ii) Apply the filtering process to the received signal, and measure the actual energy of the filtered signal, iii) Compare the expected value in i) to the measured one in ii): if the difference is larger than a given threshold, decide that the signal is present, if not, decide that the signal is absent. It must be noticed that the amplitude of the frequency response of the used filter must not be constant over the scanned band. Should this condition not met, the energy of the filtered signal is the same as the original received signal, so no conclusion could be drawn.

In order to limit the complexity of the detector while meeting the previous condition, it is proposed to use the two-tap filter $g = \frac{1}{2}[1, 1]$. Thus, the samples of the filtered signal are obtained by a simple linear interpolation of the input samples. This operation does not involve any multiplication, as a division by two is obtained by a binary shift, which limits the complexity of the filtering process. Furthermore, it can be noted that g is a low-pass filter, which guarantees that the PSD of the filtered signal is not the same as the received signal. In order to improve the performance of the presented detector, it is proposed to carry out several times the filtering process, in order to obtain different reference measures, which can be compared with the corresponding expected energy values.

It is worth mentioning that, since the proposed algorithm is based on energy measurement, the closest related detector is the usual ED. For this reason, we use the very common assumption that the noise at the output of the front-end is white and Gaussian, such as supposed in [13], [14], [17] and numerous other papers. Furthermore, we will use ED as a natural reference for performance comparison. Otherwise, the filtering processes involved in the proposed method is similar to a first-order approximation of the derivative of the received signal. Then, the suggested algorithm could be confused with the method in [21], [22], in which the derivative of the spectrum of the received signal is considered, in order to highlight discontinuities in presence of useful signal. However, the filtering processes of the proposed technique are carried out in time domain, and in frequency domain in [21], [22]. Moreover, the processes are iterative, and then not similar to a derivative in time domain.

The contributions of the paper are the following:

- To the best of the author's knowledge, the proposed detector is original, as the paradigm differs from usual ED, since the method is based on the behavior of the filtered noise in absence of useful signal. Furthermore, a simple implementation is suggested;
- The theoretical aspects of the detector are analyzed as well, as the theoretical false alarm probability, detection probability, and optimal detection threshold expressions are derived;
- The developments are supported by simulations, which show the relevance of the proposed analysis. In addition, a performance comparison with ED reveals that the proposed detector outperforms ED in SNR range of [-20-0] dB;
- Other possible applications of the method are discussed.

The remaining of the paper is organized as follows: Section 2 presents the signal model, and Section 3 describes the proposed detector. The analytical expressions of the probabilities of detection, false alarm, as well as the optimal threshold value are developed in Section 4. Simulations results are presented in Section 5, and other applications of the detector are introduced in Section 6. Finally, Section 7 concludes this paper.

2 Signal Model and Hypothesis

We consider that a sensor is scanning and sampling a frequency band with a sampling time t_s. Let y_n be the n-th sample of a received signal at the output of the receiver front-end, including analog low-pass filter, analog-to-digital converter, sub-sampling, etc. Thus, y_n can be expressed as

$$y_n = y(nt_s) = y(t)\delta(t - nt_s)\Pi_{Nt_s}, \tag{1}$$

where $y(t)$ is the received analog signal, $\delta(.)$ is the Dirac delta function, and Π_{Nt_s} is the (rectangular) observation window, with $n \in \{0, 1, .., N-1\}$. We consider the usual binary hypothesis used in signal detection, which can be written as

$$y_n = \begin{cases} \mathcal{H}_0 : & w_n \\ \mathcal{H}_1 : & r_n + w_n \end{cases}, \tag{2}$$

where $\mathcal{H}_0$ corresponds to the absence of "useful" signal, and w_n is the n-th sample of noise, which is reasonably assumed to be complex and white Gaussian $\mathcal{N}(0, \sigma^2)$ [13], [14], [17]. Under the hypothesis $\mathcal{H}_1$, the received signal r_n can be expressed with the general formulation as follows:

$$r_n = \sum_{l_c=0}^{L_c-1} h_{l_c} x_{n-l_c} e^{2j\pi\Delta_f n t_s + j\phi}, \tag{3}$$

where x_n is the transmitted signal of central frequency f_0 and bandwidth B_x, and h_n is the multipath propagation channel of length L_c. It is assumed than the signal is narrowband compared with the sensed band, namely $[f_0 - B_x/2, f_0 + B_x/2] \subset [0, \frac{1}{2t_s}]$. The term $e^{2j\pi\Delta_f n t_s}$ points out a possible frequency offset, due to channel frequency offset, and/or Doppler effect for instance. Moreover, ϕ is an unknown phase shift. Alternatively, the received signal r_n in (3) can be rewritten in the frequency domain by means of the discrete Fourier transform (DFT). Let denote by M the size of the DFT, then the m-th frequency sample, for any $m \in \{-M/2, -M/2+1, .., M/2-1\}$, can be expressed as

$$\begin{aligned} R_m &= R(f_m) \\ &= H(f_m + \Delta_f)X(f_m + \Delta_f)\mathrm{sinc}(\pi(f_m + \Delta_f)Nt_s) \\ &\times e^{-j(\pi f_m + \Delta_f)Nt_s + j\phi}, \end{aligned} \tag{4}$$

where the term $\mathrm{sinc}(\pi(f_m + \Delta_f)Nt_s)e^{-j\pi(f_m+\Delta_f)Nt_s}$ is due to the rectangular window Π_{Nt_s}. The frequency shift $f_m + \Delta_f$ is due to the convolution by $\delta(f - \Delta_f) = DFT(e^{2j\pi\Delta_f n t_s})$. Note that we do not provide any detail on the nature of the signal x_n, in order to propose a general formulation of the detector, which could be used for any kind of signal. However, we define σ_r^2 the variance of the signal r_n. Therefore, the energy of the received signal σ_y^2 can be defined according to the hypothesis as

$$\sigma_y^2 = \begin{cases} \mathcal{H}_0 : & \sigma^2 \\ \mathcal{H}_1 : & \sigma_r^2 + \sigma^2 \end{cases}. \tag{5}$$

In next section, we describe the proposed detector.

3 Proposed Detector

The basic idea behind ED is to suppose that the measured energy $\mathcal{M} = \|y_n\|^2$, where $\|.\|$ is the Euclidian norm, is statistically higher under hypothesis $\mathcal{H}_1$ than under hypothesis $\mathcal{H}_0$. If $\mathcal{M}$ is larger than a given threshold, $\mathcal{H}_1$ is decided. Then, it remains to set the best possible threshold value, in order to maximize the probability of detection. The proposed detector also uses the energy of the received signal, but is based on another paradigm. Under hypothesis $\mathcal{H}_0$, one can deduce the energy of any version of filtered noise w_n, since both the PSD of the noise and the used filter are supposed to be known *a priori*. As a consequence, it is possible to decide $\mathcal{H}_0$ by comparing the expected energy to that of the actual filtered noise. More detailed are given hereafter.

3.1 General Principle

Fig. 1 depicts the general principle of the proposed detector, compared with usual energy detector. The basic idea of the suggested algorithm is to compare two energy values:

1. a "deterministic" energy value (this value, denoted by $\tilde{\sigma}^2_{(k)}$, will be defined hereafter), which is obtained from σ_y^2. It is referred as "deterministic" as $\tilde{\sigma}^2_{(k)}$ is deduced from σ_y^2 through a predefined process.
2. the energy value of a filtered signal, the samples of which are obtained by means of an iterative filtering process with input y_n.

It will be shown afterward that the predefined "deterministic" process in Fig. 1 only depends on the filter used in the iterative process.

Based on the previous description, suppose hypothesis $\mathcal{H}_0$, then the energy of the noise w_n after the iterative filtering process is deterministic (as the filter is known). This is illustrated in Fig. 2-(a), where both the PSD of the noise and the used filter are *a priori* known. Furthermore, it is close to the energy value $\tilde{\sigma}^2_{(k)}$, by construction of the deterministic process. As a consequence, their difference should be close to zero.

In hypothesis $\mathcal{H}_1$, the energy of the filtered signal cannot be *a priori* determined, since the different features of the signal (shape, frequency, energy, etc.) are unknown. This is illustrated in Fig. 2-(b), where the cases "Signal A" and "Signal B" lead to very different measures. Therefore, unlike $\mathcal{H}_0$, it is likely that the difference between $\tilde{\sigma}^2_{(k)}$ and the energy of

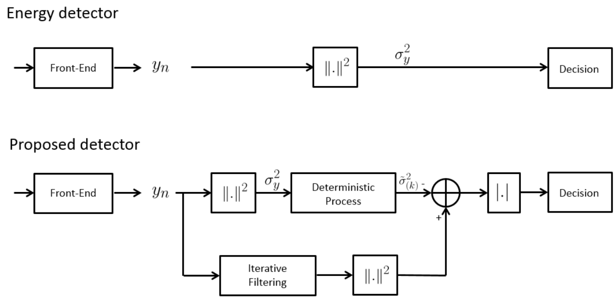

Fig. 1: General principle of the proposed detector, compared with ED.

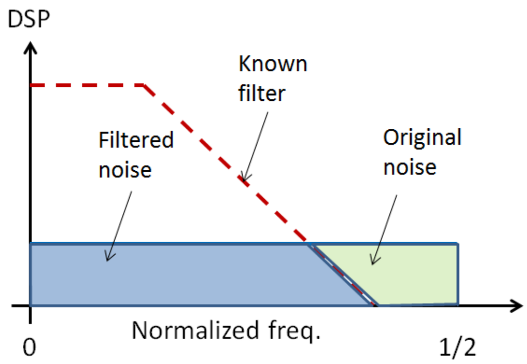

(a) Under hypothesis $\mathcal{H}_0$, the resulting energy is *a priori* known.

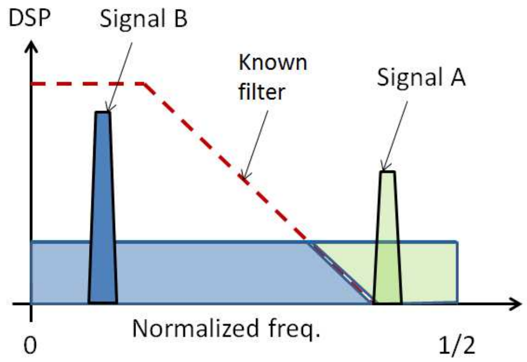

(b) Under hypothesis $\mathcal{H}_1$, the resulting energy cannot be *a priori* known.

Fig. 2: Illustration of the proposed detector: (a) in absence of signal, (b) in presence of signal.

the filtered signal largely differs from zero. This allows us to define a detector based on the energy of filtered noise.

It must be emphasized that any filter featuring a non-constant frequency response can be used in the detector. However, in order to obtain a detector with a complexity similar to ED, we propose to use the filter defined as $g = \frac{1}{2}[1, 1]$. The resulting signal samples are simply defined as the linear interpolation of two consecutive input samples. Note that the number of iterative filtering processes allows us to obtain different equivalent filter with their own cutoff frequencies, such as described in next section. Furthermore, such a filter only involves additions, since the division by two is obtained by a binary shift. Therefore, we deduce that the complexity of the proposed detector is only twice higher than that of ED, in terms of complex multiplications, which is asymptotically negligible. In the following, we provide the expression and the properties of such a signal obtained from iterative linear interpolations using $g = \frac{1}{2}[1, 1]$, and then we describe the hypothesis test.

3.2 *Iterative Linear Interpolations*

We denote by k the number of iterations of the filtering process, and $Y(k)$ the vector containing the output samples $y_n(k)$. Thus, $Y(0) = [y_0(0), y_1(0), .., y_{N-1}(0)]$ is the $\mathbb{C}^N$ vector containing the N successive samples of the received signal $y_n(0) = y_n$, and $Y(1)$ is the $\mathbb{C}^{N-1}$ vector containing the interpolated samples $y_n(1)$, where

$$y_n(1) = \frac{y_n(0) + y_{n+1}(0)}{2}. \tag{6}$$

More generally, for any $k < N$ (in practice, we will limit to $k << N$) and $n \in \{0, 1, .., N-k-1\}$, we have

$$y_n(k) = \frac{y_n(k-1) + y_{n+1}(-1)}{2} = \frac{\sum_{p=0}^{k} \binom{k}{p} y_{n+p}(0)}{2^k}. \tag{7}$$

The energy of the multi-interpolated signal $y_n(k)$ is defined as $\mathbb{E}\{y_n(k)y_n(k)^*\}$, where $\mathbb{E}\{.\}$ is the mathematical expectation. Under the hypothesis $\mathcal{H}_1$, the expression of this energy cannot be derived, since both the nature and the features of the signal are unknown (we assume a general case where r_n can be of any kind). However, under $\mathcal{H}_0$, the energy can be developed, by using the fact that the noise samples are zero-mean and independent, as follows:

$$\begin{aligned}
\mathbb{E}\{y_n(k)y_n(k)^*\} &= \mathbb{E}\{w_n(k)w_n(k)^*\} \\
&= \mathbb{E}\Bigg\{ \sum_{p_1=0}^{k} \sum_{p_2=0}^{k} \binom{k}{p_1}\binom{k}{p_2} \\
&\quad \times \frac{w_{n+p_1}(0)w_{n+p_2}(0)^*}{2^{2k}} \Bigg\} \\
&= \frac{\sum_{p=0}^{k} \binom{k}{p}^2 \sigma^2}{2^{2k}} = \tilde{\sigma}^2_{(k)}.
\end{aligned} \tag{8}$$

Alternatively, we can find $\tilde{\sigma}^2_{(k)}$ by using the frequency response of the filter. We denote by G the DFT of g such as previously defined. For convenience, we use the time-continuous version of g. Then, the M-point DFT of such a filter can be expressed as

$$\begin{aligned}
G_m = G(f_m) &= DFT(\frac{1}{2}(\delta(0) + \delta(t_s))) \\
&= e^{j\pi f_m t_s} cos(\pi f_m t_s), \\
&= e^{j\pi \frac{m}{M}} cos(\pi \frac{m}{M})
\end{aligned} \tag{9}$$

and therefore, the filter corresponding to k iterations is

$$G_{m,(k)} = G_{(k)}(f_m) = e^{j\pi \frac{km}{M}} cos^k(\pi \frac{m}{M}). \tag{10}$$

From (10), we deduce that

$$\mathbb{E}\{w_n(k)w_n(k)^*\} = \int_{-\pi/2}^{\pi/2} \frac{\sigma^2}{\pi} cos^{2k}(x)dx, \tag{11}$$

which provides in passing a demonstration of the Wallis' integral for even orders. In fact, by using the Vandermonde's identity $\sum_{p=0}^{k} \binom{k}{p}^2 = \binom{2k}{k}$, we trivially found

$$\int_0^{\pi/2} cos^{2k}(x)dx = \frac{\pi}{2}\frac{\sum_{p=0}^{k}\binom{k}{p}^2}{2^{2k}} = \frac{\pi}{2}\frac{(2k)!}{2^{2k}(k)!}. \quad (12)$$

The asymptotic expansion of the factorial, $n! \sim \sqrt{2\pi k}\left(\frac{k}{e}\right)^k$ leads to the following approximation of $\mathbb{E}\{y_n(k)y_n(k)^*\}$ under hypothesis $\mathcal{H}_0$ when k is large:

$$\mathbb{E}\{y_n(k)y_n(k)^*\} \sim \frac{\sigma^2}{\sqrt{\pi k}} \quad (13)$$

From (8) and (13), we can deduce that, under hypothesis $\mathcal{H}_0$, the energy of the k-interpolated noise can be entirely deduced from σ^2.

3.3 Hypothesis Test

Based on the previous developments, the test statistic can be expressed as

$$\mathcal{T} = \left|\frac{1}{N-k}||Y(k)||^2 - \tilde{\sigma}^2_{(k)}\right|, \quad (14)$$

where $\tilde{\sigma}^2_{(k)}$ is previously defined. Then, the usual binary decision rule is

$$\mathcal{T} \underset{\mathcal{H}_0}{\overset{\mathcal{H}_1}{\gtrless}} \eta, \quad (15)$$

where η is a threshold to be fixed, as shown in next section. Under the hypothesis $\mathcal{H}_1$, $||Y(k)||^2$ can be rewritten by using the expression of the multi-interpolated signal in the frequency domain (4). Thus, since the DFT size is $M = N - k$, we obtain

$$\frac{1}{M}||Y(k)||^2 = \frac{1}{M}\sum_{m=-M/2+1}^{M/2}|G_{m,(k)}(R_m + W_m)|^2. \quad (16)$$

In addition, we assume that $M = N - k$ is large enough to obtain the following approximation

$$\frac{1}{M}||Y(k)||^2 \approx \frac{1}{M}\sum_{m=-M/2+1}^{M/2}|G_{m,(k)}R_m|^2 + |G_{m,(k)}W_m|^2, \quad (17)$$

since the noise is zero-mean. Under the hypothesis $\mathcal{H}_0$, (17) simply becomes:

$$\frac{1}{M}||Y(k)||^2 = \frac{1}{M}\sum_{m=-M/2+1}^{M/2}|G_{m,(k)}W_m|^2, \quad (18)$$

without any approximation.

4 Deriving the False Alarm and Detection Probabilities

4.1 False Alarm Probability

In this section, we have $\sigma_y^2 = \sigma^2$ since the useful signal is absent. By definition of (8), (14) can be rewritten as

$$\begin{aligned}
\mathcal{T} &= \left|\frac{1}{M}||Y(k)||^2 - \tilde{\sigma}^2_{(k)}\right| \\
&= \left|\frac{1}{M}||Y(k)||^2 - \frac{\sum_{p=0}^{k}\binom{k}{p}^2\sigma_y^2}{2^{2k}}\right| \\
&= \left|\frac{1}{M}\sum_{m=-\frac{M}{2}+1}^{\frac{M}{2}}|G_{m,(k)}W_m|^2 - \frac{\sum_{p=0}^{k}\binom{k}{p}^2}{2^{2k}}\frac{1}{M}\sum_{m=-\frac{M}{2}+1}^{\frac{M}{2}}|W_m|^2\right| \\
&= \left|\frac{1}{M}\sum_{m=-\frac{M}{2}+1}^{\frac{M}{2}}|G_{m,(k)}W_m|^2 - \underbrace{\frac{1}{M}\sum_{p=-\frac{M}{2}+1}^{\frac{M}{2}}|G_{p,(k)}|^2}_{\Gamma_k}\frac{1}{M}\sum_{m=-\frac{M}{2}+1}^{\frac{M}{2}}|W_m|^2\right| \\
&= \frac{1}{M}\left|\sum_{m=-\frac{M}{2}+1}^{\frac{M}{2}}(|G_{m,(k)}|^2 - \Gamma_k)|W_m|^2\right|. \quad (19)
\end{aligned}$$

Let $\tilde{\mathcal{T}}$ be the variable defined as

$$\tilde{\mathcal{T}} = \frac{1}{M}\sum_{m=-\frac{M}{2}+1}^{\frac{M}{2}}(|G_{m,(k)}|^2 - \Gamma_k)|W_m|^2. \quad (20)$$

By using the Lyapounov condition for $M >> 1$, it can be proved that $\tilde{\mathcal{T}}$ has a Gaussian distribution (a detailed proof is provided in Appendix), the mean $\mu_{\tilde{\mathcal{T}}}$ and the variance $\sigma^2_{\tilde{\mathcal{T}}}$ of which are:

$$\begin{aligned}
\mu_{\tilde{\mathcal{T}}} &= \mathbb{E}\{\tilde{\mathcal{T}}\} \\
&= \frac{1}{M}\left(\sum_{m=-\frac{M}{2}+1}^{\frac{M}{2}}|G_{m,(k)}|^2 - \sum_{p=-\frac{M}{2}+1}^{\frac{M}{2}}|G_{p,(k)}|^2\right)\sigma^2 \\
&= 0, \quad (21)
\end{aligned}$$

and

$$\begin{aligned}
\sigma^2_{\tilde{\mathcal{T}}} &= \mathbb{E}\{\tilde{\mathcal{T}}^2\} \\
&= \frac{1}{M^2}\mathbb{E}\left\{\left(\sum_{m_1}\sum_{m_2}(|G_{m_1,(k)}|^2 - \Gamma_k)(|G_{m_2,(k)}|^2 - \Gamma_k) \times |W_{m_1}|^2|W_{m_2}|^2\right)\right\}. \quad (22)
\end{aligned}$$

Note that the bounds in the sum have been omitted for more readability. Since the frequency noise samples W_m are independent and identically distributed (iid), it can be noticed that

$$\sigma^2_{\tilde{\mathcal{T}}} = \underbrace{\frac{\sigma^4}{M^2}\sum_{m_1}\sum_{m_2\neq m_1}(|G_{m_1,(k)}|^2-\Gamma_k)(|G_{m_2,(k)}|^2-\Gamma_k)|W_{m_1}|^2|W_{m_2}|^2}_{=0} + \frac{2\sigma^4}{M^2}\sum_m(|G_{m,(k)}|^2-\Gamma_k)^2. \quad (24)$$

Finally, since $\tilde{\mathcal{T}} \sim \mathcal{N}(0, \sigma^2_{\tilde{\mathcal{T}}})$, then $\mathcal{T}$ obeys a Chi distribution with 1 degree of freedom, which can be expressed as

$$f_{\mathcal{T}}(x) = \sqrt{\frac{2}{\pi\sigma^2_{\tilde{\mathcal{T}}}}}\exp\Big(-\frac{x^2}{2\sigma^2_{\tilde{\mathcal{T}}}}\Big). \quad (25)$$

From (25), we deduce the expression of the false alarm probability $\mathbb{P}_{fa}$:

$$\begin{aligned}\mathbb{P}_{fa} &= \mathbb{P}(\mathcal{T} > \eta|\mathcal{H}_0)\\ &= \int_{\eta}^{+\infty} f_{\mathcal{T}}(x)\mathrm{d}x\\ &= \mathrm{erfc}\big(\frac{\eta}{\sqrt{2}\sigma_{\tilde{\mathcal{T}}}}\big), \end{aligned} \quad (26)$$

where η is a threshold that will be determined.

4.2 Detection Probability

A first remark concerns the expression of $||Y(k)||^2$ in (17). In fact, since the signal x_n is band-limited such as $2B_x \leq \frac{1}{t_s}$, then $||Y(k)||^2$ can be rewritten as

$$\begin{aligned}\frac{1}{M}||Y(k)||^2 \approx & \underbrace{\frac{1}{M}\sum_{q\in\Omega_x}|G_{q,(k)}R_q|^2}_{P_{r,k}}\\ &+ \frac{1}{M}\sum_{m=-M/2+1}^{M/2}|G_{m,(k)}W_m|^2, \end{aligned} \quad (27)$$

where Ω_x is the set of indexes corresponding to the spectral support of $x(t)$, and $P_{r,k}$ is the energy of the interpolated received signal.

4.2.1 Detection Probability for Deterministic Signal: In a first approach, we assume that the signal is deterministic, i.e. both h_n nor x_n are deterministic processes. In that case, $P_{r,k}$ is a constant, and the test $\mathcal{T}$ can be expressed as

$$\mathcal{T} = \frac{1}{M}\underbrace{\Bigg|P_{r,k} + \sum_{m=-\frac{M}{2}+1}^{\frac{M}{2}}(|G_{m,(k)}|^2-\Gamma_k)|W_m|^2\Bigg|}_{\tilde{\mathcal{T}}}, \quad (28)$$

where $\tilde{\mathcal{T}} \sim \mathcal{N}(P_{r,k}, \sigma^2_{\tilde{\mathcal{T}}})$. The cumulative distribution function (cdf) of $\mathcal{T}$ can then be derived as

$$\begin{aligned}F_{\mathcal{T}|\mathcal{H}_1}(x) &= \mathbb{P}(\mathcal{T} \leq x)\\ &= \mathbb{P}(x \leq \tilde{\mathcal{T}} \leq x)\\ &= \int_{-x}^{x}\frac{1}{\sqrt{2\pi\sigma^2_{\tilde{\mathcal{T}}}}}\exp\Big(-\frac{(x-P_{r,k})^2}{2\sigma^2_{\tilde{\mathcal{T}}}}\Big)\mathrm{d}x\\ &= \frac{1}{2}\Big(-\mathrm{erf}\Big(\frac{-x+P_{r,k}}{\sqrt{2\sigma^2_{\tilde{\mathcal{T}}}}}\Big) + \mathrm{erf}\Big(\frac{x+P_{r,k}}{\sqrt{2\sigma^2_{\tilde{\mathcal{T}}}}}\Big)\Big). \end{aligned} \quad (29)$$

The probability of detection is expressed from (29) as

$$\begin{aligned}\mathbb{P}_d &= \mathbb{P}(\mathcal{T} \geq \eta|\mathcal{H}_1)\\ &= 1 - F_{\mathcal{T}|\mathcal{H}_1}(\eta). \end{aligned} \quad (30)$$

4.2.2 Detection Probability for Gaussian Random Signal: If it is supposed that R_q obeys a Gaussian random process, then $P_{r,k}$ has a Gaussian distribution, the mean and variance of which are

$$\mu_P = \frac{1}{M}\sum_{q\in\Omega_x}|G_{q,(k)}|^2\mathbb{E}\{|R_q|^2\}, \quad (31)$$

where $\mathbb{E}\{|R_q|^2\}$ is the energy of the received signal before any interpolation, and without noise contribution, and

$$\sigma^2_P = \frac{1}{M^2}\sum_{q_1\in\Omega_x}\sum_{q_2\in\Omega_x}|G_{q_1,(k)}|^2|G_{q_2,(k)}|^2\mathbb{E}\{|R_{q_1}|^2|R_{q_2}|^2\}. \quad (32)$$

As a consequence, $\tilde{\mathcal{T}}$ (which is defined as previously) is a sum of two uncorrelated Gaussian variable, then $\tilde{\mathcal{T}} \sim \mathcal{N}(\mu_P, \sigma^2_P + \sigma^2_{\tilde{\mathcal{T}}})$, and finally, the cdf of $\mathcal{T}$ is

$$\begin{aligned}F_{\mathcal{T}|\mathcal{H}_1}(x) &= \mathbb{P}(\mathcal{T} \leq x)\\ &= \frac{1}{2}\Big(-\mathrm{erf}\Big(\frac{-x+\mu_P}{\sqrt{2(\sigma^2_P+\sigma^2_{\tilde{\mathcal{T}}})}}\Big)\\ &\quad + \mathrm{erf}\Big(\frac{x+\mu_P}{\sqrt{2(\sigma^2_P+\sigma^2_{\tilde{\mathcal{T}}})}}\Big)\Big). \end{aligned} \quad (33)$$

Finally, the probability of detection is expressed exactly as in (30).

4.3 Threshold Value η

We here suppose that the threshold value is set according to the false alarm probability $\mathbb{P}_{fa}$ (it could be equivalently set according to the detection probability $\mathbb{P}_d$). Thus, from (26), we deduce that from a desired (target) $\mathbb{P}_{fa}$ value, we find η by solving (inverting) (26), i.e.

$$\eta = \sqrt{2}\sigma_{\tilde{\mathcal{T}}}\mathrm{erfc}^{-1}(\mathbb{P}_{fa}). \quad (34)$$

We deduce from (34) and (24) that, in addition to the target pfa, the optimal threshold value depends on the noise variance and the number of samples M. This particularity is similar to the energy detector. The specificity of the proposed detector is that the η value also depends on the number of interpolations, which appears in the expression of $\sigma_{\tilde{\mathcal{T}}}$.

5 Simulations Results

The aims of the presented simulations results are 1) to validate the previous analytical results, and 2) to compare the performance of the proposed detector with that of the usual ED. In fact, both detectors are energy-based methods, therefore agnostic to the received signals, and have similar complexity. To show the latter assertion, from Section 3, we deduce that the proposed detector requires the following operations:

- $\tilde{\sigma}^2_{(k)}$: N multiplications and N additions;
- $||Y(k)||^2$: M multiplication, since the multiplications by $\frac{1}{2}$ in the filtering processes are "costless" in term of complexity, and $kM + M$ additions.

Then, since $N >> k$ we approximate $M \approx N$, hence the computation cost of $\mathcal{T}$ in (14) is $2N$ multiplications and $(k+1)N$ additions. The complexity of ED is N multiplications and N additions, then we deduce that the proposed detector is of the same order of complexity as that of ED.

5.1 Validation of Theoretical Developments

In Fig. 3 is depicted the η value versus the false alarm probability. The results obtained through simulation are compared with those obtained with (34), for different SNR values (-20 to -5 dB). Furthermore, $N = 1000$ samples are used, and $k = 4$ iterations. It can be clearly observed that theoretical results match with simulations, which validates the previous developments.

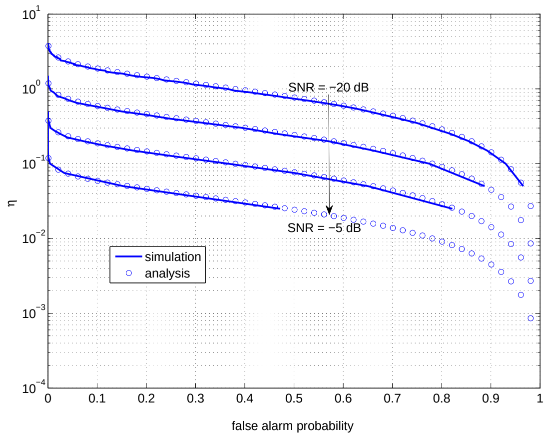

Fig. 3: η versus the false alarm probability. Comparison of the simulations and the analysis (34).

5.2 ROC Performance

The performance of the proposed detector is analyzed through the receiver operating characteristic (ROC), and is compared with the energy detector. Fig. 4 shows the spectrum $|Y(f)|$ of the received signal in absence and in presence of the noise, for a SNR of -10 dB (in all simulations, the signal energy has been normalized). The considered signal in Fig. is OFDM with 1000 subcarriers of 1 kHz each. It can be seen that the signal is concealed in noise.

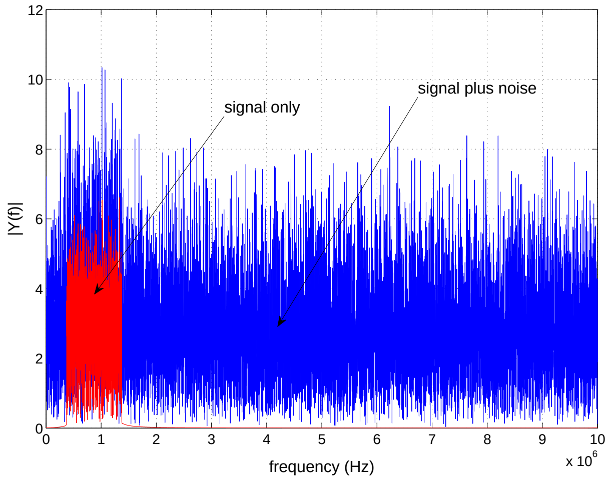

Fig. 4: Spectrum $|Y(f)|$ of the received signal in absence and in presence of the noise, SNR=-10 dB. The signal is OFDM.

First series of simulation shows the ROC performance of the detector, considering the previous OFDM signal, in absence of channel. In all the simulations, the proposed detector is used with ten iterations. The central frequency of the signal has been randomly (uniformly) chosen in the interval $[500, 9500]$ kHz. Fig. 5 depicts the ROC performance of the proposed detector compared with energy detector, by using $N = 1000$ samples. Figs. 5-(a), (b), and (c) correspond to SNRs of -10, -15, and -20 dB, respectively. It can be observed that the proposed detector outperforms the energy detector for SNR=-10 and -15 dB, and both achieves almost the same performance at SNR=-20 dB.

Other series of simulations have been carried out in order to compare the proposed method to ED. Results are presented in Fig. 6. The same observations as previously can be drawn from Fig. 6-(a), where $N = 10000$: the proposed detector outperforms the energy detector at both SNR=-15, and -20 dB. Obviously, both detectors achieve better performance in Fig. 6-(a) than in Fig. 5, due to the larger number of samples.

In Fig. 6-(b), we compare the performance of the proposed detector with the ED in presence of a Rayleigh channel. The SNR is set to -15 dB. It can be observed that the proposed detector still outperforms the energy detector. Moreover, both of them achieve a slightly weaker performance than in AWGN, due to the presence of the channel. Then, the simulations results show that, with similar computation cost, the proposed detector outperforms ED.

Fig. 6-(c) shows the ROC performance of the proposed detector for different kinds of signals: sinusoid, OFDM, and chirp. The SNR has been set to -15 dB, and the sensing duration corresponds to $N = 1000$ samples. The detector performs better when applied to sinusoid than OFDM, and when applied to OFDM than chirp. This result is mainly due to the bandwidth of the different signals: the narrowest the signal bandwidth, the better the performance of the detector.

6 Other Possible Applications

6.1 Estimation of the Parameters f_0 and Δ_f

It has been aforementioned that the multiple interpolations act like a low-pass filter. Under several conditions, it becomes possible to estimate the parameters f_0 and Δ_f in presence of useful signal r_n. In fact, it must be pointed out that the largest k, the lowest the "cutoff frequency" of $G_{m,(k)}$. Therefore, according to f_0, and assuming that $B_x << \frac{1}{t_s}$, it may

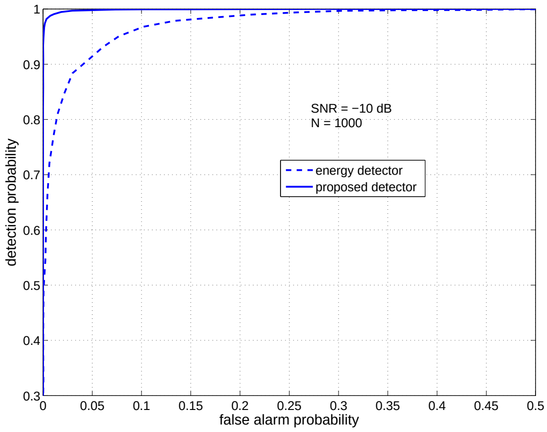

(a) SNR=-10 dB.

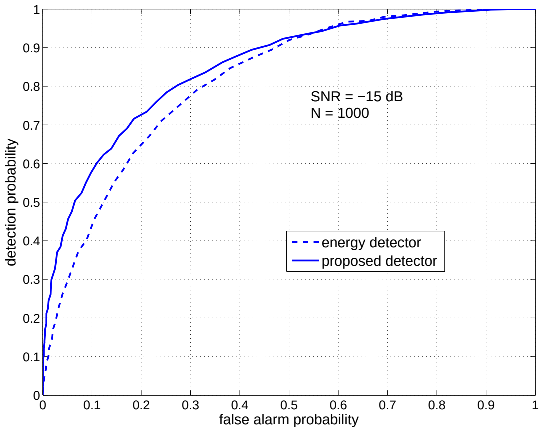

(b) SNR=-15 dB.

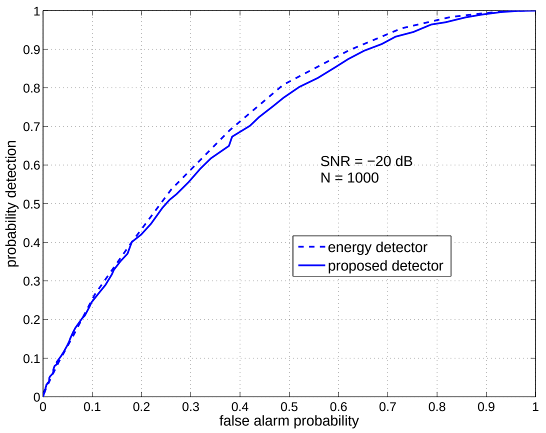

(c) SNR=-20 dB.

Fig. 5: ROC performance of the proposed detector compared with energy detector, $N = 1000$.

happen that for a given $k = k_1$, we have $\frac{1}{M}||Y(k)||^2 > \tilde{\sigma}^2_{(k)}$ (when f_0 is lower than the cutoff frequency of $G_{m,(k_1)}$), and for $k = k_2 > k1$, we have $\frac{1}{M}||Y(k)||^2 < \tilde{\sigma}^2_{(k)}$ (when f_0 is much larger than the cutoff frequency of $G_{m,(k_2)}$).

As a consequence of the above remark, it exists $k^* \in \mathbb{R}^*_+$ and $k_1 < k^* < k_2$, such as $\frac{1}{M}||Y(k^*)||^2 = \tilde{\sigma}^2_{(k^*)}$. Note that k^* has no physical sense since it may be not an integer. However it is possible, mathematically speaking, to extend k^* from integer to real domain. In practice, k^* corresponds to the point where the linearly-interpolated trajectories of $||Y(k)||^2$ and $\tilde{\sigma}^2_{(k)}$ intersect.

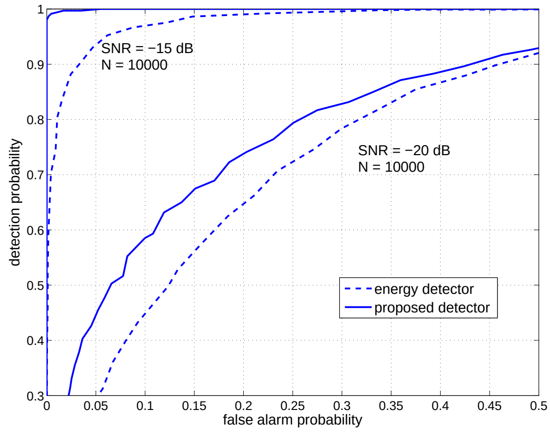

(a) $N = 10000$, SNR=-15 and -20 dB.

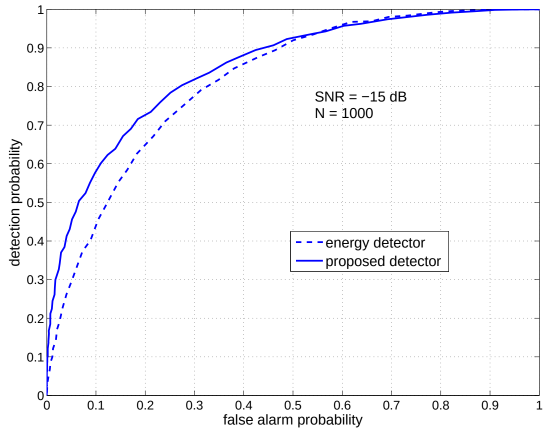

(b) $N = 10000$, in presence and absence of Rayleigh channel.

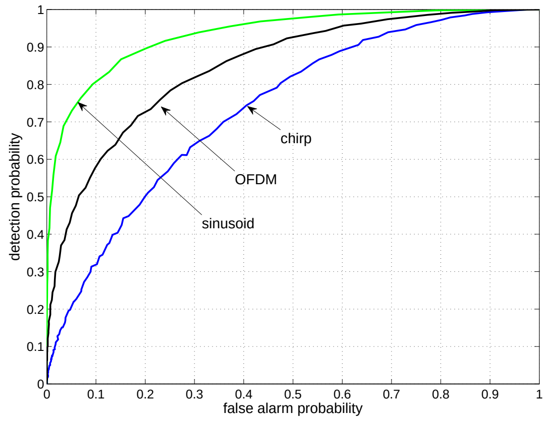

(c) Comparison for different signal kinds, $N = 1000$ in AWGN channel.

Fig. 6: ROC performance of the proposed detector compared with energy detector, for various parameters.

In order to estimate f_0 and Δ_f, some conditions must be assumed:

• The signal is narrow-band with $B_x << \frac{1}{t_s}$.
• As a consequence, we suppose that $|R_q| = C$ (C is a constant) for any q in Ω_x.
• The values $\frac{1}{M}||Y(k)||^2$ has been computed for every k value, in such a way that k^* has been estimated.
• N is large enough to consider that the approximation

$$\frac{1}{M}\sum_m |G_{m,(k)}W_m|^2 \approx \frac{\sum_{p=0}^{k}\binom{k}{p}^2\sigma^2}{2^{2k}}$$

holds.

Furthermore, for a clarity purpose, we note $f_{0,\Delta} = f_0 + \Delta_f$. According to the above assumption and using (27), the equality $\frac{1}{M}||Y(k^*)||^2 = \tilde{\sigma}^2_{(k^*)}$ leads to

$$\begin{aligned}
&\frac{1}{M}\sum_{q\in\Omega_x}|G_{q,(k^*)}R_q|^2 + \frac{1}{M}\sum_{m=-M/2+1}^{M/2}|G_{m,(k^*)}W_m|^2 \\
&= \frac{\binom{2k^*}{k^*}}{2^{2k^*}}(\sigma_r^2+\sigma^2) \\
&\Leftrightarrow \frac{1}{M}\sum_{q\in\Omega_x}|G_{q,(k^*)}R_q|^2 = \frac{\binom{2k^*}{k^*}}{2^{2k^*}}\frac{1}{N}\sum_{q\in\Omega_x}|R_q|^2 \\
&\Leftrightarrow \sum_{q\in\Omega_x}|G_{q,(k^*)}|^2 C = \frac{\binom{2k^*}{k^*}}{2^{2k^*}}\frac{M|\Omega_x|C}{N} \\
&\Leftrightarrow \sum_{q\in\Omega_x^+}|G_{q,(k^*)}|^2 = \frac{\binom{2k^*}{k^*}}{2^{2k^*+1}}\frac{M|\Omega_x|}{N},
\end{aligned} \tag{35}$$

where $\binom{2k^*}{k^*} = \Gamma(2k^*+1)/\Gamma(k^*+1)^2$. Since $|G(\pi x)|$ is a strictly decreasing function for any $x \in [0,1]$, then it exists a unique Ω_x^+ which is the solution of (35). Finally, since $f_{0,\Delta}$ is the (scaled) central frequency of the signal, then it can be estimated as

$$\hat{f}_{0,\Delta} = \frac{\max(\Omega_x^+) + \min(\Omega_x^+)}{2}\frac{1}{Mt_s}. \tag{36}$$

Furthermore, if f_0 is known in advance, then Δ_f can be estimated by

$$\hat{\Delta}_f = \hat{f}_{0,\Delta} - f_0. \tag{37}$$

6.2 Detection of Colored Noise

It is possible to take advantage of the nature of low-pass filter linear interpolator to detect colored noise, and to decide whether it is pink or blue noise. In that case, the detection hypothesis can be rewritten as

$$y_n = \begin{cases} \mathcal{H}_0: & w_n \\ \mathcal{H}_1: & \bar{w}_n \end{cases}, \tag{38}$$

where $\bar{w}_n$ is the colored sample. The decision test (15) remains, but the detector decides whether the noise is white or colored. Furthermore, it can detect the kind of color, by applying the test:

$$\frac{1}{M}||Y(k)||^2 - \tilde{\sigma}^2_{(k)} \underset{\text{blue}}{\overset{\text{pink}}{\gtrless}} 0. \tag{39}$$

Fig. 7 shows the trajectories of $||Y(k)||^2$ in cases of pink, white, and blue noises versus the number of interpolations. Since the white noise corresponds to the case $\frac{1}{M}||Y(k)||^2 \approx \tilde{\sigma}^2_{(k)}$, the test statistic (39) can be verified from Fig. 7.

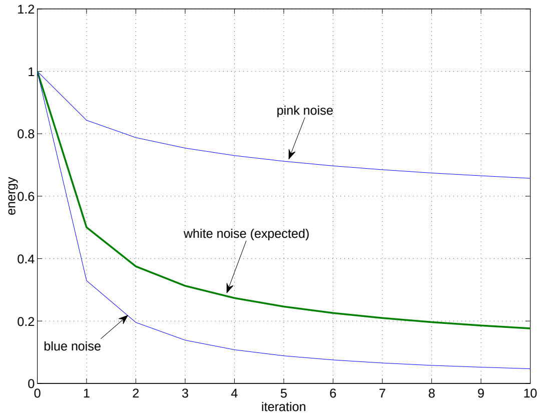

Fig. 7: Trajectories of the energy of interpolated pink, white, and blue noises versus the number of interpolations.

7 Conlusion

In this paper, we have presented a new detector of narrow-band signals in noise, based on the difference of a deterministic function of the energy of the signal and the energy of the filtered signal. Unlike ED, the proposed detector consists in exploiting the behavior of the energy of filtered white noise, which can be *a priori* determined since the used filter is known. Thus, if the measured energy differs from an expected value, it is decided that the signal is present in the band. In order to reduce the complexity of the method, it has been proposed to use a simple two-tap filter. The false alarm and detection probabilities expressions have been derived, as well as the optimal threshold value. Furthermore, theoretical results have been verified through simulations. It has been shown that the new detector outperforms the usual ED. Finally, two other possible applications of the detector have been presented. Future work will consist in investigating these pending issues, and to analyze the inherent limits of the proposed detector due to noise uncertainty.

References

7.1 Journal articles

[3] Ren, Q.: 'Energy Detection Performance Analysis for UWB Radar Sensor Networks', EURASIP Journal on Wireless Communications and Networking, 2010, 2010, pp. 1–16

[5] Yücek, T., Arslan, H.: 'A Survey of Spectrum Sensing Algorithms for Cognitive Radio Applications', IEEE Communications Surveys and Tutorials, 2009, 6, (1), pp. 116–130

[6] Zeng, Y., Liang, Y.-C., Hoang, A. T., et al.: 'Review on Spectrum Sensing for Cognitive Radio: Challenges and Solutions', EURASIP Journal on Advances in Signal Processing, December 2010, 2010, pp. 1–15

[7] Lu, L., Zhou, X., Onunkwo, U., et al.: 'Ten years of research in spectrum sensing and sharing in cognitive radio', EURASIP Journal on Wireless Communications and Networking, January 2012, 2012, (28), pp. 1–16

[8] Axell, E., Leus, G., Larsson, E. G., et al.: 'Spectrum Sensing for Cognitive Radio: State-of-the-Art and Recent Advances', IEEE Signal Processing Magazine, May 2012, 29, (3), pp. 101–116

[9] Gardner, W. A.: 'Exploitation of Spectral Redundancy in Cyclostationary Signals', IEEE Signal Processing Magazine, April 1991, 8, (2), pp. 14–36

[12] Zeng, Y., Liang, Y.-C.: 'Spectrum Sensing Algorithms for Cognitive Radio Based on Statistical Covariances', IEEE Trans. on Vehicular Technology, May 2009, 58, (4), pp. 1804–1815

[15] Tandra, R., Sahai, A.: 'SNR Walls for Signal Detection', IEEE Journal of Selected Topics in Signal Processing, February 2008, 2, (1), pp. 4–17

[16] Jouini, W.: 'Energy Detection Limits under Log-Normal Approximated Noise Uncertainty', IEEE Signal Processing Letters, July 2011, 18, (7), pp. 423–426

[17] Mariani, A., Giogetti, A., Chiani, M.: 'Effects of Noise Power Estimation on Energy Detection for Cognitive Radio Applications', IEEE Trans. on Communications, December 2011, 59, (12), pp. 3410–3420

[20] Moghimi, F., Schober, R., Mallik, R. K.: 'Hybrid Coherent/Energy Detection for Cognitive Radio Networks', IEEE Trans. on Wireless Communications, June 2011, 10, (5), pp. 1594–1605

[22] Guibène, Turki, M., W., Hayar, A.: 'Spectrum sensing for cognitive radio exploiting spectrum discontinuities detection', EURASIP Journal on Wireless Communications and Networking, January 2012, 2012, (4), pp. 1–9

7.2 Conference Paper

[2] Bhargavi, D., Murthy, C. R.: 'Performance comparison of energy, matched-filter and cyclostationaritybased spectrum sensing'. Proc. SPAWC'10, Marrakech, Morocco, June 2010, pp. 1–5

[4] Pevtsov, G., Yatsutsenko, A., Trofimenkos, Y., et al.: 'Theoretical basics of radar signals energy detection', Proc. MMET'12, Kyiv, Ukraine, August 2012

[10] Lunndén, J., Koivunen, V., Huttunen, A., et al.: 'Spectrum Sensing in Cognitive Radios Based on Multiple Cyclic Frequencies', Proc. CROWNCOM'07, Orlando, USA, August 2007, pp. 37–43

[11] Cardoso, L. S., Debbah, M., Bianchi, P., et al.: 'Cooperative Spectrum Sensing Using Random Matrix Theory', Proc. ISWPC'08, Santorini, Greece, May 2008, pp. 1–5

[18] Shukla, S., Rao, A. K., Srivastava, N.: 'A Survey on Energy Detection Schemes in Cognitive Radios', Proc. ICETEESES'16, Sultanpur, India, March 2016, pp. 223–228

[19] Khalaf, Z., Nafkha, A., Palicot, J., et al.: 'Hybrid Spectrum Sensing Architecture for Cognitive Radio Equipment', Proc. AICT'10, Barcelona, Spain, May 2010, pp. 46–51

[21] Guibène, W., Hayar, A., Turki, M.: 'Distribution Discontinuities Detection using Algebraic Technique for Spectrum Sensing in Cognitive Radio', Proc. CROWNCOM'10, Cannes, France, June 2010, pp. 1–5

7.3 Book, book chapter and manual

[1] Proakis, J., Salehi, M.: 'Digital Communications' (McGraw-Hill, 2008, 5th edn. 2008)

[13] Atapattu, S., Tellambura, C., Jiang, H.: 'Chapter 2: Conventional Energy Detector', in: 'Energy Detection for Spectrum Sensing in Cognitive Radio' (Springer, 2014, 1st edn.), pp. 11–26

[14] Oppenheim, A. V., Verghese, G. C.: 'Chapter 14: Signal Detection', in: 'Introduction to Communication, Control, and Signal Processing' (MIT Courses, 2010), pp. 247–261

8 Appendices

In this appendix, we prove that, for $M >> 1$, $\tilde{\mathcal{T}}$ in (20) has a Gaussian distribution. Let $X_m = \frac{1}{M}(|G_{m,(k)}|^2 - \Gamma_k)|W_m|^2$ (in (20)) be a random variable, which obeys a Chi-squared distribution with two degrees of freedom. The Lyapounov condition states that: if the $2+\alpha$-th moment (with $\alpha > 0$) of independent variables X_m exists, the mean μ_m and the variance σ_m^2 are finite, and if

$$\lim_{M \to +\infty} \frac{r_M}{s_M} = 0, \tag{40}$$

where

$$r_M^{2+\alpha} = \sum_{m=1}^{M} \mathbb{E}\{|X_m - \mu_m|^{2+\alpha}\}, \tag{41}$$

and

$$s_M^2 = \sum_{m=1}^{M} \sigma_m^2, \tag{42}$$

then $\sum_m = X_m$ tends toward a Gaussian distribution, the mean and the variance of which are (21) and (24). In the following, we set $\alpha = 2$. Note that, due to the symmetry of $|G_{m,(k)}|^2$, we can limit to the positive index of m. It is straightforward to show that

$$\mu_m = \frac{1}{M}(|G_{m,(k)}|^2 - \Gamma_k)\sigma^2, \tag{43}$$

$$\sigma_m^2 = \frac{\sigma^4}{M^2}(|G_{m,(k)}|^2 - \Gamma_k)^2, \tag{44}$$

and

$$\mathbb{E}\{|X_m - \mu_m|^4\} = \frac{9\sigma^8}{M^4}(|G_{m,(k)}|^2 - \Gamma_k)^4. \tag{45}$$

Let define $\mathbf{G}$ the $\mathbb{R}^M$ vector which contains the elements $|G_{m,(k)}|^2 - \Gamma_k$, then we can rewrite $\frac{r_M}{s_M}$ in (40) as

$$\frac{r_M}{s_M} = 9^{1/4}\frac{||\mathbf{G}||_4}{||\mathbf{G}||_2}, \tag{46}$$

where $||.||_4$ and $||.||_2$ are the 4-norm and the Euclidian norm, respectively. We now prove that the ratio of the two norm in (46) tends to zero when M tends to the infinity.

Proof: Let $p : [x_l, x_u] \mapsto [-1, 1]$ be a function of class C^1 on the interval $[x_l, x_u]$, where $(x_l, x_u) \in \mathbb{R}^2$ and are finite number. Let f^- and f^+ two piecewise linear functions on $[x_l, x_u]$ such as, $\forall x \in [x_l, x_u]$, we have

$$\begin{cases} f^-(x) \le p(x) \le f^+(x), & \text{if } p(x) \ge 0 \\ f^-(x) \ge p(x) \ge f^+(x), & \text{if } p(x) \le 0 \end{cases}. \tag{47}$$

Fig. 8 illustrates the above definition of $f^-(x)$ compared with $p(x)$. In this example $p(x)$ is the cos function.

In the following, we only focus on f^-, as the developments remain the same for f^+. We suppose that f^- is defined on N_I distinct intervals $I_i = [x_i, x_{i+1}]$ such, such that for any $1 \le i \le N_I$ and $x \in I_i$, we have

$$f^-(x) = a_i x + b_i, \tag{48}$$

where $|a_i| < +\infty$ and $|b_i| < +\infty$, since p is of class C^1 on $[x_l, x_u]$.

We define $\mathbf{F}^-$ and $\mathbf{P}$ two vectors of size M, which correspond to the regularly sampled versions of f^- and p on $[x_l, x_u]$, respectively. For a sake of simplicity, but without loss

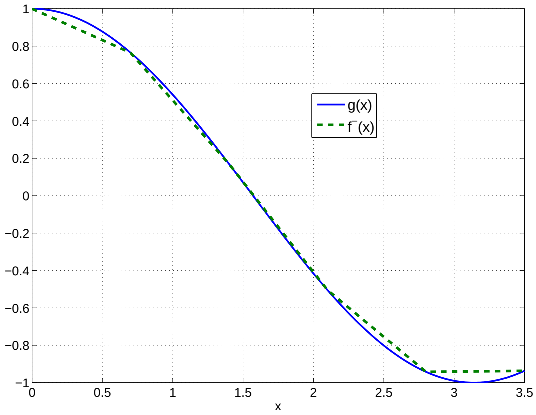

Fig. 8: Illustration of $p(x)$ and $f^-(x)$.

of generality, we suppose that any element p_m of $\mathbf{P}$ is positive. As a consequence, for any $m = 1, .., M$, we can write

$$0 \le f_m^- = p_m - \epsilon_m \le p_m, \tag{49}$$

where ϵ_m is a real positive value. By definition of the sampling process, f_m^- can be expressed as

$$f_m^- = a_i(x_l + (m-1)\frac{x_u - x_l}{M-1}) + b_i. \tag{50}$$

The first step of the proof is to show that it is possible to find $\mathbf{F}^-$ such that

$$\begin{aligned} & \frac{||\mathbf{F}^-||_4}{||\mathbf{F}^-||_2} \ge \frac{||\mathbf{P}||_4}{||\mathbf{P}||_2} \\ \Leftrightarrow\ & \frac{||\mathbf{F}^-||_4^4}{||\mathbf{F}^-||_2^4} \ge \frac{||\mathbf{P}||_4^4}{||\mathbf{P}||_2^4} \\ \Leftrightarrow\ & \frac{\sum_m (p_m - \epsilon_m)^4}{(\sum_m (p_m - \epsilon_m)^2)^2} \ge \frac{||\mathbf{P}||_4^4}{||\mathbf{P}||_2^4}. \end{aligned} \tag{51}$$

To this end, we analyzes the gradient of $\frac{||\mathbf{F}^-||_4^4}{||\mathbf{F}^-||_2^4}$. For any $1 \le m \le M$, we define the function $V(\epsilon_m)$ as

$$V(\epsilon_m) = \frac{\overbrace{\sum_{k \ne m} (p_k - \epsilon_k)^4}^{A} + (p_m - \epsilon_m)^4}{\Big(\underbrace{\sum_{k \ne m} (p_k - \epsilon_k)^2}_{B} + (p_m - \epsilon_m)^2\Big)^2}, \tag{52}$$

the derivative of which is

$$\begin{aligned} \frac{\partial V(\epsilon_m)}{\partial \epsilon_m} = & \frac{1}{\big(B + (p_m - \epsilon_m)^2\big)^3} \times \\ & 4(p_m - \epsilon_m)\Big(A - B(p_m - \epsilon_m)^2\Big). \end{aligned} \tag{53}$$

From (53), we deduce that the numerator of $\frac{\partial V(\epsilon_m)}{\partial \epsilon_m}$ is null for $\epsilon_m \in \{p_m - \sqrt{\frac{A}{B}}, p_m, p_m + \sqrt{\frac{A}{B}}\}$. Moreover, a straightforward analysis shows that

$$\frac{\partial V(\epsilon_m)}{\partial \epsilon_m} \geq 0, \text{ if } p_m - \sqrt{\frac{A}{B}} \leq \epsilon_m \leq p_m \quad (54)$$

$$\frac{\partial V(\epsilon_m)}{\partial \epsilon_m} \leq 0, \text{ if } p_m \leq \epsilon_m \leq p_m + \sqrt{\frac{A}{B}}. \quad (55)$$

Therefore, $V(\epsilon_m)$ reaches a local minimum at $\epsilon = p_m - \sqrt{\frac{A}{B}}$, and a local maximum at $\epsilon = p_m$. It can be noted that:

1. $0 \leq \epsilon_m \leq p_m$ (from (49)),
2. Since $|p| \leq 1$, then $A \leq B$, hence it can be straightforwardly shown that $V(0) \leq V(p_m)$

As a consequence of the above remarks, we deduce that, for any $1 \leq m \leq M$, it is ever possible to find ϵ_m, $p_m \geq \epsilon_m \geq p_m - \sqrt{\frac{A}{B}}$ if $p_m - \sqrt{\frac{A}{B}} \geq 0$ or $p_m \geq \epsilon_m \geq 0$ if $p_m - \sqrt{\frac{A}{B}} \leq 0$ such that $V(\epsilon_m) \geq V(0)$. Therefore it exists a vector $\boldsymbol{\epsilon}$ containing the elements ϵ_m, $\mathbf{F}^- = \mathbf{P} - \boldsymbol{\epsilon}$, such that (51) holds.

From the above result, we can now provide an upper bound of $\frac{||\mathbf{P}||_4}{||\mathbf{P}||_2}$. In fact, when M is large, then from (50):

$$\begin{aligned} ||\mathbf{F}^-||_2 &= \left(\sum_m |f_m^-|^2\right)^{1/2} \\ &\sim \left(\sum_m \beta_2 \frac{m^2}{M^2}\right)^{1/2} \\ &\sim \left(\frac{\beta_2 M}{3}\right)^{1/2}, \end{aligned} \quad (56)$$

since the sum of the M first terms in m^2 is equivalent to $\frac{M^3}{3}$. The term β_2 is the sum of $(a_i(x_u - x_l))^2$ and. The same reasoning leads to

$$\begin{aligned} ||\mathbf{F}^-||_4 &= \left(\sum_m |f_m^-|^4\right)^{1/4} \\ &\sim \left(\sum_m \beta_4 \frac{m^4}{M^4}\right)^{1/4} \\ &\sim \left(\frac{\beta_4 M}{5}\right)^{1/4}, \end{aligned} \quad (57)$$

since the sum of the M first terms in m^4 is equivalent to $\frac{M^5}{5}$, and β_4 is a constant independent of M. Therefore, we deduce that, when M is large enough:

$$\frac{\beta_4^{1/4} 3^{1/2}}{\beta_2^{1/2} 5^{1/4} M^{1/4}} \geq \frac{||\mathbf{P}||_4}{||\mathbf{P}||_2}, \quad (58)$$

which concludes the proof.